International Journal of Nanomedicine

Dovepress
open access to scientific and medical research

Open Access Full Text Article

ORIGINAL RESEARCH

Carbon Dots Derived from Os Draconis and Their Anxiolytic Effect

Yumin Chen[1], Wei Xiong[2,3], Ying Zhang[1], Xue Bai[1], Guoliang Cheng[1], Yifan Zhang[1], Rui Chen[1], Yinghui Guo[1], Hui Kong[1], Yue Zhang[4], Huihua Qu[5], Yan Zhao[1]

[1]School of Traditional Chinese Medicine, Beijing University of Chinese Medicine, Beijing, People's Republic of China; [2]School of Chinese Materia Medica, Beijing University of Chinese Medicine, Beijing, People's Republic of China; [3]Institutes of Health Research, Mayinglong Pharmaceutical Group Co., Ltd, Wuhan, Hubei, People's Republic of China; [4]School of Life Sciences, Beijing University of Chinese Medicine, Beijing, People's Republic of China; [5]Centre of Scientific Experiment, Beijing University of Chinese Medicine, Beijing, People's Republic of China

Correspondence: Yan Zhao, School of Traditional Chinese Medicine, Beijing University of Chinese Medicine, No. 11 Bei San Huan Dong Lu, Chaoyang District, Beijing, People's Republic of China, Email zhaoyandr@163.com; Huihua Qu, Centre of Scientific Experiment, Beijing University of Chinese Medicine, No. 11 Bei San Huan Dong Lu, Chaoyang District, Beijing, People's Republic of China, Email quhuihuadr@163.com

Background: At present, people are susceptible to developing depression and anxiety disorders in response to stress. However, there is no specific medicine for anxiety. Os Draconis (OD, named "Long gu" in Chinese) are fossilized bones that have been used in traditional Chinese medicine to treat neurological diseases for thousands of years. Thus, we conducted this study to determine the biological basis for the anxiolytic effect of OD.

Methods: In this study, novel carbon dots (OD-CDs) from OD decoctions were discovered and separated. OD-CDs were anatomized using nanomaterials characterization methods to characterize the morphological structure, optical properties, and functional group properties. Four behavioural tests were conducted to observe the behavioural activities of mice, including the open field test (OFT), light/dark box test (LDT), elevated plus maze test (EPMT), and novelty-suppressed feeding test (NSFT), to determine its anxiolytic effects. Moreover, we assessed the possible mechanisms of the OD-CDs by detecting hormones associated with the hypothalamic-pituitary-adrenal (HPA) axis.

Results: OD-CDs were spherical and monodispersed with a narrow size distribution between 1 and 5 nm and had a yield of 3.67%. OD-CDs increased the activity time of mice in the central zone in the OFT. The mice in the experimental group showed more frequent activity in the light compartment and the open arms, in LDT and EPMT, respectively. In addition, OD-CDs shortened the feeding latency in the NSFT. Furthermore, the results after OD-CDs intervention showed a significant increase in serum serotonin (5-HT) and norepinephrine (NE). In addition, the concentrations of corticotropin-releasing hormone (CRH), adrenocorticotropic hormone (ATCH), and corticosterone (CORT) were decreased.

Conclusion: These results demonstrate a definite anxiolytic effect of OD-CDs and reveal the possible mechanism of action of OD-CDs' anxiolytic effect, which supports the research of OD for neurological disorders and a promising new trend of therapeutic approach and drug development.

Keywords: Os Draconis, carbon dots, anti-anxiety, HPA axis

Introduction

Anxiety disorders are among the most common neuropsychiatric disorders affecting all age groups in modern life. Because the incidence of anxiety disorders has been constantly growing,[1–3] it has become a global problem; the WHO ranked anxiety disorders as the ninth leading health-related cause.[4] Anxiety disorders are often closely associated with depression, whose mechanisms have not yet been clarified. Benzodiazepines have been widely used to treat several forms of anxiety. However, these compounds have well-known side effects, such as amnesia, muscle relaxation, and dependence potential.[5] Currently, the commonly used and effective anti-anxiety drugs are primarily selective serotonin reuptake inhibitors (SSRIs) and serotonin noradrenaline reuptake inhibitors (SNRIs). Although both can reduce patients' anxiety symptoms to some extent, these drugs often require a long duration of treatment over weeks. The occurrence of

Received: 14 July 2022
Accepted: 3 October 2022
Published: 20 October 2022

Graphical Abstract

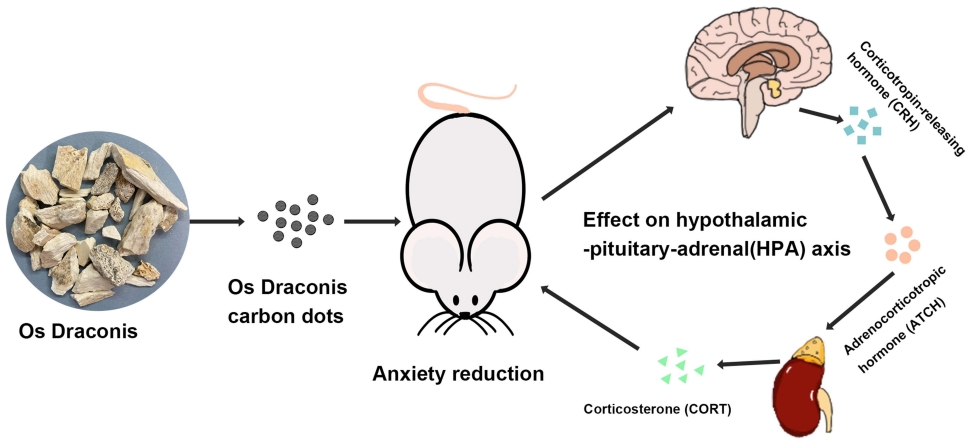

possible early exacerbation of symptoms and adverse reactions, for instance, emotional abnormalities, withdrawal reactions, and suicidal tendencies affect patient compliance. Such a situation has prompted the research of other more effective and safer anxiolytic drugs.[6,7]

As a member of nanomaterials, carbon dots (CDs) were first discovered during the purification of single-walled carbon nanotubes via preparative electrophoresis in 2004.[8] Due to its special structure and characteristics, it has become a hot spot for research because of its biological effects on the body. As a new carbon source, the preparation of charcoal medicine has a long history in Chinese medicine, and the extraction of nanocomponents from it is facile, economical, simple, and easy to synthesize.[9–11] Our research team has found a variety of carbon dots from herbal charcoal medicines that have different pharmacological activities. For instance, semi-carbonized nanodots derived from *Atractylodes macrocephala* show a positive anti-gastric ulcer effect.[12] Carbon dots derived from *Crinis Carbonisatus* (CrCi-CDs) exert neuroprotective effects by reducing neuroexcitatory toxicity.[13] It follows that some nanoparticles have a therapeutic effect on neurogenic diseases. For example, aggregated single-walled carbon nanotubes attenuate the impact of methamphetamine on behaviour and neurochemistry in mice.[14] Other studies have found the distribution of carbon nanoconstituents in the nervous system and its neuroprotective effects.[15,16]

Os Draconis (OD), named "Long gu" in Chinese, is a traditional fossilized medicine used widely as a tranquilizer in China. It was originally described in "Shennong's Herbal Classic of Materia Medica", which was written before the Han Dynasty, and used for over 2000 years in traditional Chinese medicine (TCM).[17,18] Moreover, pharmacological studies and considerable clinical research have shown that OD could be used to treat neurological diseases, such as anxiety, depression, and insomnia.[19] OD has been shown to have anti-anxiety effects but the material basis has not yet been elucidated. Still there are few reports on whether the carbon dots inside Os Draconis are active substances. This led us to further study this new substance and confirmed carbon dots (CDs). For the first time, we found nanoparticles in the OD.

In this study, we separated and characterized Os Draconis carbon dots (OD-CDs) from the OD. Furthermore, we evaluated the anxiolytic effect of OD-CDs and found underlying anxiolytic mechanisms through animal behavioural tests.

Materials and Methods

Chemicals

OD was purchased from BEI JING Qian Cao Traditional Chinese Medicine Co., Ltd (Beijing, China). Diazepam (DZP) was purchased from Yimin Pharmaceutical Factory (Beijing, China). A dialysis membrane with a 1000 Da molecular weight cut-off (MWCO) was obtained from Beijing Ruida Henghui Technology Development Co., Ltd (Beijing, China).

CCK-8 was purchased from Dojindo Molecular Technologies, Inc. (Kumamoto, Japan). The CCK-8 assay was obtained from Dojindo Molecular Technologies, Inc. (Kumamoto, Japan). Enzyme-linked immunosorbent assay (ELISA) kits measuring the concentrations of serotonin (5-HT), norepinephrine (NE), corticotropin-releasing hormone (CRH), adrenocorticotropic hormone (ATCH), and corticosterone (CORT) were purchased from Cloud-Clone Corp. (Katy, TX, USA). All experiments were performed using deionized water (DW).

Animals

Male ICR mice (25.0 ± 2.0 g) were purchased from SPF (Beijing) Biotechnology Co., Ltd. All mice were maintained under the following conditions: ambient temperature, 24.0 ± 1.0 °C, relative humidity 55–65%, and a 12-h light/dark cycle with *ad libitum* access to food and water. Food was withdrawn from the mice 60 min before drug treatment. Behavioural experiments were performed in a quiet laboratory between 17:00–22:00. The experimental procedures were approved by the Committee of Ethics of Animal Experimentation of Beijing University of Chinese Medicine (BUCM) and by the Health Guide for Care and Use of Laboratory Animals.

Preparation of OD-CDs

First, the OD was smashed into a fine powder in a grinder (SL-500A, Zhejiang Song Qing Metal Technology Co., Ltd., China). Next, fine OD powder was soaked in DW and boiled three times for 1 h to separate and obtain the OD decoction. Finally, the resulting solution was filtered to remove residues, concentrated, and dialyzed with DW for 96 h using a 1000 Da MWCO dialysis membrane to purify the OD-CDs. All the purification procedures for the OD-CDs were performed using DW. The entire preparation process for the OD-CDs is shown in Figure 1.

Characterization of OD-CDs

The morphology and microstructure of OD-CDs were characterized by transmission electron microscopy (TEM, Tecnai G2 20, FEI Company, OR, USA) at an accelerating voltage of 200 kV. The structural details and the atomic lattice fringes of OD-CDs were examined by high-resolution TEM (HRTEM, JEN-1230, Japan Electron Optics Laboratory, Japan), transmission electron microscopy (TEM), and high-resolution TEM.

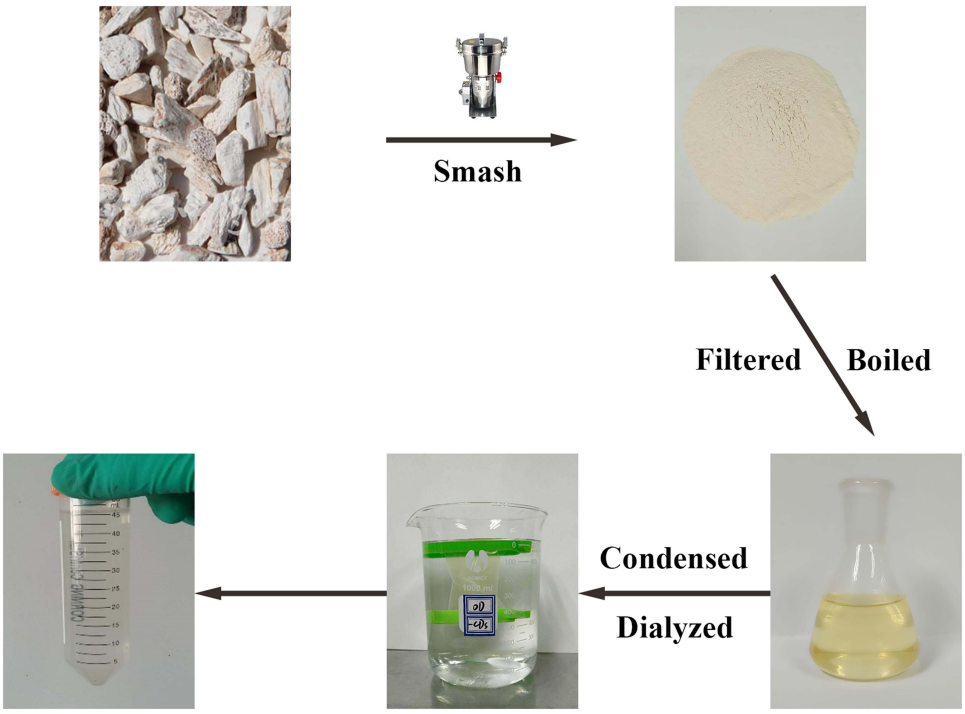

Figure 1 Flow diagram of the Os Draconis carbon dots (OD-CDs) preparation process.

The spectral properties of the OD-CDs were investigated using ultraviolet-visible spectroscopy (UV-vis, CECIL, Cambridge, UK) and fluorescence spectroscopy (F-4500, Tokyo, Japan) in a standard quartz cuvette. Moreover, the Fourier transform infrared (FTIR, Thermo, California, USA) spectra were recorded to analyse the organic functional groups in the OD-CDs within a spectral window of 400–4000 cm^{-1}. Raman spectra were acquired by using a Renishaw (in Via plus) Raman microscope with 785 nm wavelength incident laser light. To obtain X-ray diffraction (XRD) patterns, an X-ray diffractometer (D8-Advanced X-ray diffractometer, Bruker AXS, Karlsruhe, Germany) with Cu Kalpha radiation was applied. The surface composition and elemental analysis of the OD-CDs were recorded using X-ray photoelectron spectroscopy (XPS, ESCALAB 250 Xi, Thermo Fisher Scientific, Fremont, CA, USA) and a mono X-ray source Al Kl excitation (1486.6 eV).

Quantum Yield (QY) of OD-CDs

The fluorescence QY of the OD-CDs was measured using quinine sulfate (% QY was 54 in a 0.1 M sulfuric acid [H_2SO_4] solution) as a standard sample and calculated using the following equation:

$$Q_{CDs} = Q_R \times \frac{I_{CDs}}{I_R} \times \frac{A_R}{A_{CDs}} \times \frac{\eta^2_{CDs}}{\eta^2_R}$$

where "Q" represents "QY", "I" is the integrated area under the emission spectrum, "A" is the absorbance at 350 nm wavelength, and "η" is the refractive index of the solvent.[20] The subscripts "CDs" and "R" refer to the OD-CDs and standard, respectively. To minimize the reabsorption effect, the A_R and A_{CDs} were maintained below 0.05.

Behavioural Tests

Male mice were assigned to perform the behavioural tests. Each group was used in one of the tests, the open-field test (OFT), light/dark box test (LDT), elevated plus maze test (EPMT), and novelty-suppressed feeding test (NSFT), with no mice being exposed to more than once. Animals were habituated to experimental conditions 60 min before testing. Animals were injected intraperitoneally as indicated: control (normal saline [NS]), DZP (2 mg/kg), and low-dose -, medium-, and high OD-CDs (10, 20, and 40 mg/kg, respectively). All the behavioural tests were performed on the 7th day of pretreatment. On Day 8, OD-CDs and DZP treatment were administered 50 and 30 min, respectively, before behavioural tests. After each experiment, the apparatus was thoroughly cleaned with 75% ethanol to obviate any possible bias caused by odour cues from previous animals.

Open Field Test

The OFT apparatus was a nontransparent container (50 cm × 50 cm × 30 cm), with a black floor divided into 25 zones (10 cm × 10 cm). The container was illuminated by a 60 W floor lamp, which provided illumination in the testing room only. On the ceiling, a digital camera controlled by the computer was placed 2.6 m above the centre of the container. The 16 zones that were adjacent to the walls represented a safe area (peripheral area), and the 9 zones in the centre represented an exposed area (central area). Each mouse was individually placed in the centre of the container and allowed to explore the container freely for 5 min.[21] In addition to locomotor activity, time spent in the centre area of the open field, and total movement distance parameters were assessed to index anxiety levels.[22] The OFT test was recorded using a digital camera on the ceiling and videos were analysed using EthoVision XT 7 software (Noldus Information Technology, Wageningen, Netherlands).

Light/Dark Box Test

The LDT apparatus was a rectangular Plexiglas box (60 cm × 45 cm × 35 cm) divided into light and dark compartments, with 1/3 transparent and 2/3 printed black. The transparent compartment was lit using a 60 W lamp. These compartments were separated by a baffle with a square opening (4 cm × 4 cm) at floor level.[23,24] Each mouse was individually gently placed in the centre of the light compartment, facing the opening. Each animal was video monitored for 5 min and the time spent in the light compartment was analysed.[25]

Elevated Plus Maze Test

The EPMT apparatus mainly consisted of two nontransparent opposite open arms (30 cm × 5 cm) and two opposite closed arms (30 cm × 5 cm × 25 cm) in a cross configuration. The arms were connected to a central platform (5 cm × 5 cm), and the apparatus was elevated 45 cm above the floor. The maze was illuminated by a 60 W floor lamp. A digital video was suspended above the maze to record the movements of the mice. Each mouse was gently placed in the centre of the platform facing an open arm, video recorded for 5 min. The ratio of time spent in open arms [(open arm times/total times) × 100] was calculated from video recordings to study the anxiolytic-like activity in the mice.[26] If a mouse fell from the maze, it was removed from the experiment.

Novelty-Suppressed Feeding Test

Because of the contradiction between the anxiety of the experimental animals (due to being in a new environment) and the drive of food temptation, the degree of anxiety can be judged according to the latency of approaching and eating the food, which is described as an essential method for the study of the efficacy of anti-anxiety drugs.[27,28] Five identical arenas (40 cm ×40 cm ×30 cm) were placed in a quiet and bright environment, with a red piece of paper of the same size placed in the centre of the arena where a piece of feed was positioned on. Mice were tested after 24 h of fasting. When starting, mice were placed from one corner of the arena and the time taken to approach the food with the first bite was recorded. The cut-off time was 300 s for each mouse. At the end of each experiment, the paper and feed were replaced and the arenas were cleaned with 75% alcohol.

Neurotransmitter and HPA Hormone Assay

Serum and Brain Tissue Collection

After the behavioural tests, the mice were allowed to recover for 24 h before blood collection. On Day 8, OD-CDs were administered 50 min and DZP 30 min before sample collection. Blood samples were collected into a centrifuge tube and allowed to clot for 2 h at room temperature, and later centrifuged for 10 min at 3000 r/min at 4 °C to obtain serum. After blood collection, brain tissue was carefully peeled out of the hippocampus and cerebral cortex in mice after decapitation on ice. Samples were stored at −80 °C for subsequent factor analysis.

Neurotransmitter and HPA Hormone Detection

The concentrations of 5-HT, NE, CRH, ATCH, and CORT were determined using an enzyme-linked immunosorbent assay (ELISA) method. Mouse ELISA kits were used according to the manufacturer's instructions. The optical density (OD) was measured at a wavelength of 450 nm using a microplate reader (Biotek, VT, USA).

Cell Viability Assay

The cytotoxicity of OD-CDs was assessed in RAW 264.7 cells using a CCK-8 assay.[29] Cells were cultured in Dulbecco's modified Eagle's medium (DMEM) supplemented with 20% foetal bovine serum in a humidified 5% CO_2 atmosphere. The temperature of the incubation environment was maintained at 37 °C. Cells were counted and seeded in 96-well plates at a density of 1×10^5/well with 100 μL medium per well. After incubation for 24 h, 100 μL with varying concentrations of OD-CDs (10,000, 5000, 2500, 1250, 625, 312.5, 156.25, 78.13, and 39.06 μg/mL) was added to the designated wells. Next, cells with OD-CDs were cultured for 24 h. Following this, cells were washed twice with PBS, and 100 μL/well CCK-8 solution (V_{CCK-8}: VDMEM=1:9) was added for an additional 4 h incubation. Finally, a microplate reader (Biotek, Winooski, VT, USA) was used to detect the optical density (OD) of each well at a wavelength of 450 nm. Cell viability was calculated using the following formula:

Cell viability (% of control) = (Ae-Ab/Ac-Ab) × 100.

Ae, Ab, and Ac represent the A450 of the experimental, blank, and control groups, respectively. The experiments were performed on three independent samples.

Statistical Analysis

Statistical analyses were performed using the statistical package for the social sciences (SPSS, version 19.0, Chicago, IL, USA). Normally distributed data with equal variances are expressed as the mean ± standard deviation. Multiple comparisons were performed using a one-way analysis of variance (ANOVA) followed by the least significant difference test. Nonnormally distributed data are expressed as the median (quartile range). The within-group differences were assessed using a nonparametric test, while a Wilcoxon signed-rank test was used to compare two groups. Data were plotted using a box plot. $P < 0.05$ and $P < 0.01$ were considered statistically significant.

Results

Characterization of OD-CDs

As shown in Figure 2A, the typical TEM image of the OD-CDs showed that CDs with an average particle diameter of 2.75 nm (Figure 2B) were nearly spherical and well separated from each other. Furthermore, as shown in Figure 2C, the HRTEM image revealed that CDs had a lattice spacing of 0.233 nm.

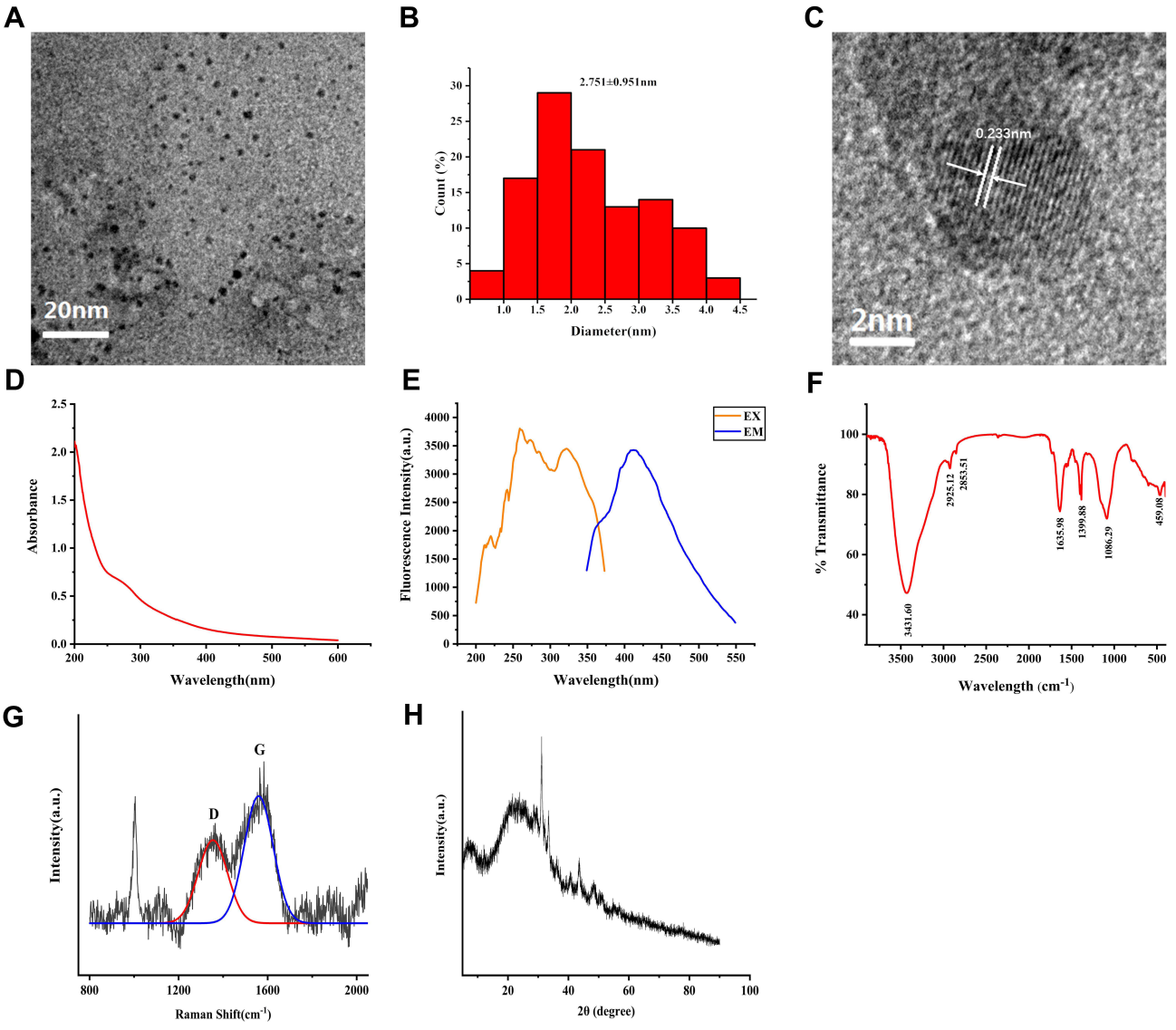

Figure 2 Characterization of Os Draconis carbon dots (OD-CDs). (**A**) Transmission electron microscopy (TEM) image. (**B**) TEM size distribution. (**C**) High-resolution TEM (HRTEM) image. (**D**) Ultraviolet-visible (UV-vis). (**E**) Fluorescence spectra and spectrum. (**F**) Fourier transform infrared spectroscopy (FTIR) spectrum. (**G**) Raman spectrum. (**H**) X-ray diffraction pattern.

The aqueous OD-CDs solution exhibited a broad absorption spectrum, and had a weak adsorption peak at 270 nm, which can be ascribed to the π–π* transition of the aromatic C=C bond by UV-vis absorption spectroscopy (Figure 2D).[30] The fluorescence spectra of OD-CDs show a maximum emission at 470 nm with excitation at 357 nm (Figure 2E). The QY of the OD- CDs was determined to be 3.67%.

The FT-IR spectra were acquired to determine the surface and functional groups. CD-CDs exhibited characteristic peaks at 3431 cm^{-1}, 2925 cm^{-1}, 2853 cm^{-1}, 1635 cm^{-1},1399 cm^{-1},1086 $cm^{-1,}$ and 459 cm^{-1} in the purified OD-CDs (Figure 2F). The peak at 3431 cm^{-1} was assigned to O–H bonds, while peaks at 2925 cm^{-1} and 2853 cm^{-1} reflected C–H bonds. The peak at 1635 cm^{-1} was assigned to C=O bands. Small bands at 1399 cm^{-1} reflected C-N stretching, while the broad peak at 1086 cm^{-1} indicated C–O stretching.

Figure 2G shows the D band (peak at 1354 cm^{-1}) and G band (peak at 1559 cm^{-1}) regions of OD-CDs by the Raman spectrum, and the latter is related to the vibration of sp^2-bonded carbon atoms. The intensity ratio of the D and G bands (I_D/I_G) was 0.66, which indicates higher content of amorphous carbon in OD-CDs.[31]

XRD spectrum showed a distinct diffraction peak for OD-CDs (2θ=22.765°), indicating that OD-CDs are mainly amorphous carbon and the atomic lattice spacing was 0.390 nm by using MDI Jade 6 software. Also, it showed that OD-CDs probably present crystal structures associated with Ca elements in the spectrum (Figure 2H).

The surface composition and elemental analysis of the prepared OD-CDs were characterized by the XPS technique. The result showed that there are four peaks at 284.8, 531.8, 399.8, and 347.3eV (Figure 3A) corresponding to C 1s, O 1s, N 1s, and Ca 2p, respectively. The OD-CDs were primarily composed of carbon (44.87%), oxygen (36.11%), nitrogen (2.75%), and calcium (3.65%). The high-resolution XPS spectrum of C 1s (Figure 3B) can be resolved into four peaks with binding energies at 284.9,285.8, 287.0, and 289.2 eV, which reflected the C-C/C=C, C-O, C=O and C=N bonds, respectively. The O 1s spectrum (Figure 3C) was deconvoluted into three peaks at 532.8, 531.8, and 530.9 eV, which were assigned to O-C=O, C-OH, and C=O, respectively. The N 1s spectrum (Figure 3D) was fitted with three peaks at 399.5, 400.1, and 400.3 eV, which were attributed to N=C, C-N-C, and N-$(C)_3$ bonds, respectively.[32,33] In addition, the Ca 2p XPS spectrum can be curve fitted into two peak components at approximately 347.4 eV and 351.0 eV (Figure 3E), attributed to Ca $2p_{3/2}$ and $2p_{1/2}$ respectively.[34]

Behavioural Tests in Mice Treated with OD-CDs

Open Field Test

As shown in Figure 4B, diazepam (DZP) and high-, medium-, and low-dose OD-CDs increased the time spent in the OFT central area (31.17 ± 6.29 s, 23.11 ± 5.09 s, 20.54 ± 12.05 s, respectively) compared with the control group (19.63 ± 3.31 s). Analysis revealed that DZP ($P < 0.05$) and high-dose OD-CDs ($P < 0.01$) significantly increased the time spent in the OFT central area compared with the control group. However, as seen in Figure 4A, DZP and high-, medium- and low-dose OD-CDs did not significantly change the locomotion distance. The data indicate that the OD-CDs may not significantly impact their motor activity. Mice in the diazepam and OD-CDs groups had more complex activity trajectories and traversed the central zone more frequently than the control group (Figure 4C).

Light/Dark Box Test

In addition, we tested five groups of mice using LDT. A 7-day administration with DZP and high-, medium-, and low-dose OD-CDs increased the time spent in the light compartment (218 ± 21.35 s, 206 ± 32.17 s, 196 ± 28.46 s, 174 ± 24.36 s, respectively) compared with the control group. Furthermore, OD-CDs significantly increased the time spent in the light compartment ($P < 0.01$, Figure 4D).

Elevated Plus Maze Test

The results of EPMT showed that a 7-day administration of high-, medium-, and low-dose OD-CDs significantly increased the time spent in open arms (24.75 ± 3.76 s, 24.87 ± 3.37 s, 21.31 ± 5.43 s, respectively) compared with the control group (11.47 ± 3.06 s). Post hoc analysis revealed that all doses of OD-CDs significantly increased the ratio of time spent in the open arms of the elevated plus-maze test compared with the control group, as shown in Figure 4E ($P < 0.01$). This result indicated that the OD-CDs may improve the exploratory activity of the mice. From the roadmap and

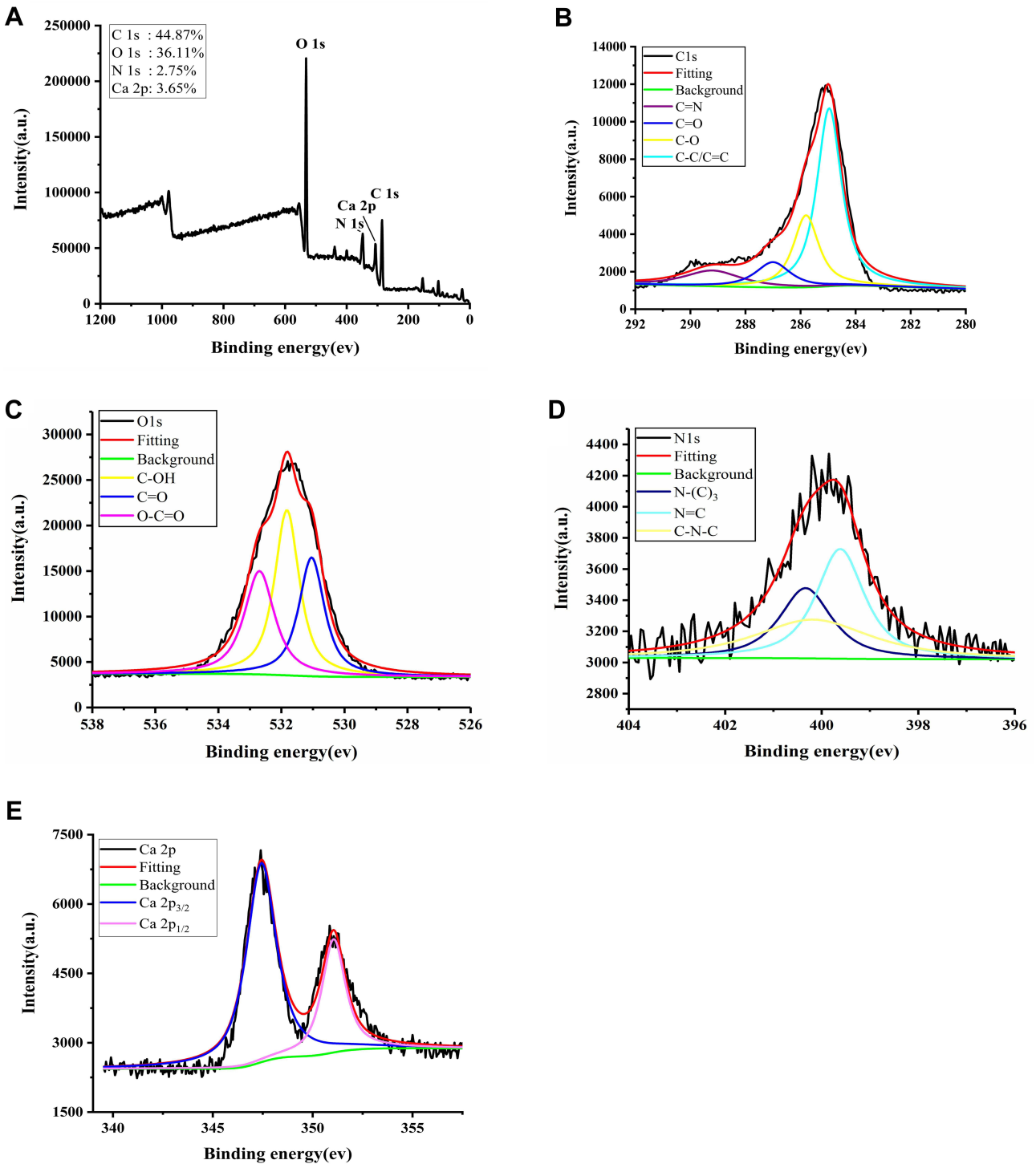

Figure 3 Surface composition and elemental analysis of Os Draconis carbon dots (OD-CDs) by X-ray photoelectron spectroscopy (XPS). (**A**) XPS full scan spectrum, and high-resolution spectra of (**B**) C 1s, (**C**) O 1s, (**D**) N 1s, and (**E**) Ca 2p.

heatmap of the mouse trajectory, the control group mice tended to be more likely to stay in the closed arms of the left and right sides and had a propensity to explore the open arms. The mice in the diazepam group favoured staying in the central zone and spent a higher proportion of time in the open arm. Similarly, mice in the OD-CDs groups also displayed more exploratory behaviour in the open arm (Figure 4F and G).

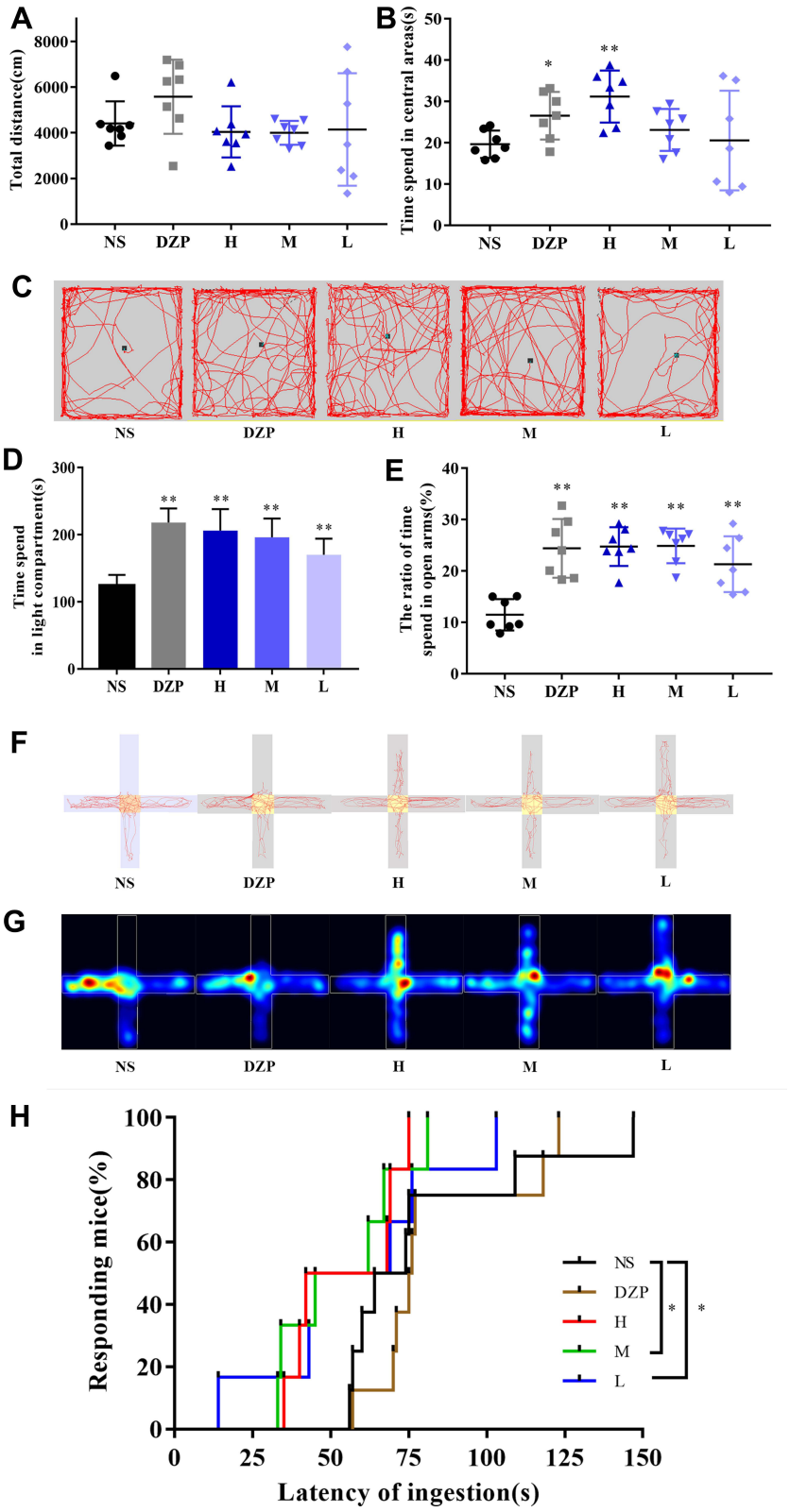

Figure 4 Effect of Os Draconis carbon dots (OD-CDs) on behavioural tests in ICR mice. (**A**) The total distance travelled in the open-field test (OFT), and the time spent in the central area (**B**). (**C**) Path diagram of open-field exploration in mice. (**D**) Time spent in a light compartment in the light/dark box test (LDT). (**E**) The ratio of time spent in the open arms in the elevated plus maze test (EPMT). (**F**) Path diagram of elevated plus maze activity in mice. (**G**) Heatmap representations of mouse activity in the elevated plus maze. (**H**) The cumulative percentage of animals that ingested (latency to eat) in the novelty-suppressed feeding test (NSFT). The mice were treated with normal saline (NS), diazepam (DZP), and high (**H**), medium (**M**), and low (**L**) doses of OD-CDs, n = 7/group. $^{**}P < 0.01$ and $^{*}P < 0.05$ compared with the control group.

Novelty-Suppressed Feeding Test

In the NSFT (Figure 4H), the feeding latency of mice in the control (80.75±31.64 s) and diazepam (83.38±23.79 s) groups approximated without no significant difference after 7 days of gavage, while the latency in the OD-CDs (H 56.8 ±815.58 s, M 56.50±17.22 s, L55.38±26.45 s, respectively) group was significantly shortened, with a significant difference in the medium- and low-dose groups compared with the control group ($P < 0.05$).

Concentrations of Neurotransmitters and HPA Hormones Following OD-CDs Treatment

After 7 days of drug treatment with OD-CDs at three doses, the serum 5-HT concentration increased in mice when compared with the control group, with the largest increase shown with the medium-dose treatment (Figure 5A). Treatment with high-dose OD-CDs significantly increased the NE concentration when compared with the control groups. There were no significant differences in NE concentration between the low, medium, and control groups (Figure 5B). The concentrations of CRH, ACTH, and CORT were significantly decreased by treatment with high-dose OD-CDs (Figure 5C–E) compared with the control group.

We simultaneously examined 5-HT levels in the hippocampus and cerebral cortex of mice to determine whether OD-CDs affect the level of 5-HT in the brain tissue of mice. Based on Figure 5F, the concentration of 5-HT in the diazepam group was not significantly different from that in the control group ($P > 0.05$). Nevertheless, the high ($P < 0.05$) and medium ($P < 0.01$) doses of OD-CDs significantly elevated the concentration of 5-HT in the cerebral cortex, while the medium dose also enhanced the concentration of 5-HT in the hippocampus ($P < 0.05$).

In vitro Cytotoxicity

Figure 6 shows the cell viability of RAW 264.7 cells treated with OD-CDs at eight concentrations at 10,000, 5000, 2500, 1250, 625, 312.5, 156.25, 78.13, and 39.06 μg/mL for 24 h. The OD-CDs did not influence RAW 264.7 cell growth at concentrations up to approximately 1250 μg/mL. RAW 264.7 cells viability gently decreased as the CD concentration increased from 1250 to 10,000 μg/mL, indicating that the cytotoxicity of OD-CDs was negligible below 1250 μg/mL.

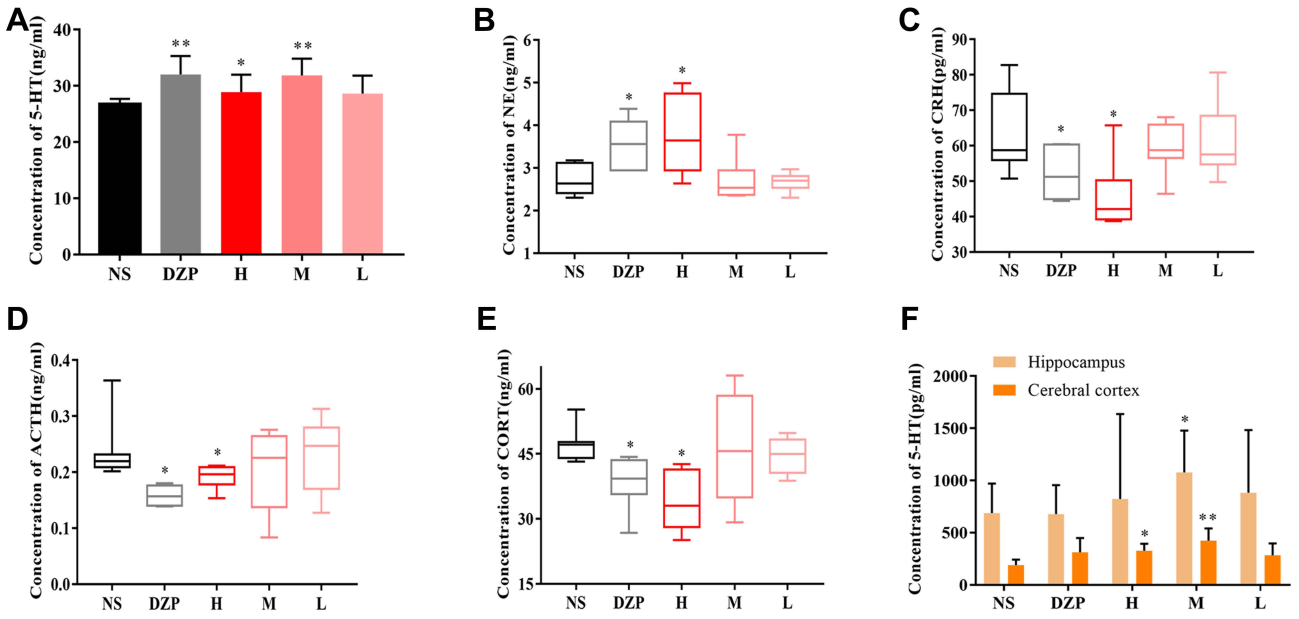

Figure 5 Effect of Os Draconis carbon dots (OD-CDs) on serum 5-HT, NE, CRH, ATCH, and CORT concentrations. (**A**) Serum concentration of 5-HT, (**B**) NE, (**C**) CRH, (**D**) ACTH, and (**E**) CORT. (**F**) The concentration of 5-HT in the hippocampus and cerebral cortex. Mice were treated with normal saline (NS), diazepam (DZP), and different doses of OD-CDs: high (**H**), medium (**M**), and low (**L**), n = 7/group. $^{**}P < 0.01$ and $^{*}P < 0.05$ compared with the control group.

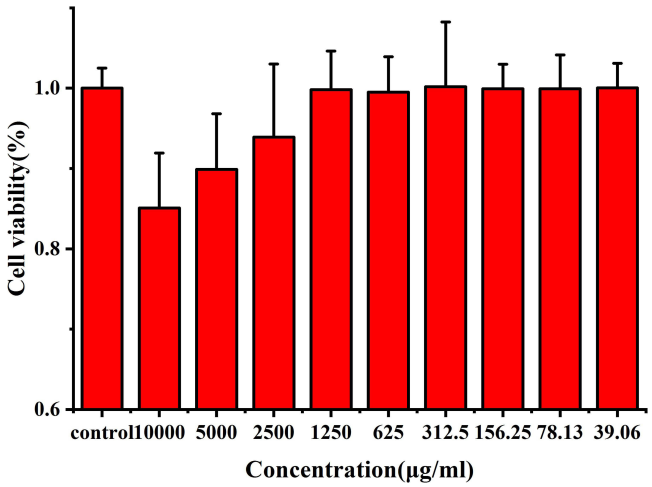

Figure 6 Cell viability of RAW 264.7 cells after incubation with various concentrations of Os Draconis carbon dots (OD-CDs) for 24 h.

Discussion

As a commonly used mineral drug in TCM, fossilized bones of ancient mammals such as rhinoceroses, deer, cattle, elephants, etc., OD has a long history of clinical applications for the treatment of neuropsychiatric disorders. Supported by clinical evidence, the antianxiety effect of OD is explicit. Although the constituents of OD that have been described in previous studies showed that OD mainly contains a large proportion of calcium elements and a variety of amino acids,[35] studies on the effective site of sedation and anxiolysis of OD are scant. The isolation and purification of the effective components of the anxiolytic effect in OD and the preliminary study of their mechanism of action are the concerns of this research.

Anxiety or fear can be induced by experiencing a novel environment that can be assessed in animals by determining the intensity of behaviour in an unacquainted area.[36] We utilized several classical animal tests including the OFT, LDT, EMPT, and NSFT to evaluate the effect of OD-CDs on anxiety-like behaviours in mice. These behavioural tests have excellent reliability and validity and are routinely used to assess anxiolytic activity in rodents.[37,38] In these four tests, mice were introduced to the new environment and could not escape, which induced a state of anxiety. Previous studies have shown that increased time spent in the central area in the OFT, light compartment in the LDT and open arms of the EPMT, and less time of latency to eat is one indicator of the effectiveness of anti-anxiety drugs.[39,40] Our study found that compared with NS, administration of OD-CDs for 7 days resulted in significant anti-anxiety effects, close in potency to diazepam, a typical benzodiazepine drug that is often used in the animal model of anxiety as a positive control drug and has a clinically stable antianxiety effect.[41,42] DZP did not have sedative effects at 2 mg/kg.[43] To avoid the possibility of a false-positive effect, OD-CDs were evaluated for their effects on the total distance moved during the OFT. We found that OD-CDs (10–40 mg/kg) did not have any significant effect on locomotor activity. This indicated that the increase in the time spent in the OFT central area, light compartment, and open arm and the shorter latency to ingestion were caused by an anxiolytic-like, nonsedative effect.

On the one hand, nanoparticles may exert neuroprotective effects by modulating the inflammatory response and reducing ROS.[44,45] The other nanoscale drugs were found to improve anxiety symptoms via the gut-brain axis,[46] neurotransmitters, or other pathways.[47] Research indicates that nanoparticles can enter and exit the biological barrier via exosome transfer, which is the pathway through the blood-brain barrier for many nanomedicines to exert their neurotherapeutic effects.[48–50] Based on our results, OD-CDs modified neurotransmitters and serum hormones in anxious mice.

The pathogenesis of anxiety disorders is complex. Many hypotheses have been proposed, such as the monoamine neurotransmitter and the hypothalamus-pituitary-adrenal (HPA) axis hypotheses.[51,52] The monoamine neurotransmitter hypothesis has been widely studied. 5-HT and NE signalling pathways are a basic index of most current clinical anxiolytics and are an important system for evaluating anxiolytic components. In addition, clinical treatment has

shown that the concentration of 5-HT or NE gradually increases with the administration of anxiolytics, which also indicates the improvement of symptoms.[53] Thus, we sought to confirm the anxiolytic effects of the OD-CDs by measuring the concentration of these factors. Our results showed that high-, medium- and low-dose OD-CDs and DZP significantly increased the concentration of serum 5-HT. The 5-HT concentration in the brain differs tremendously from that in serum, with a sharp correlation with mood regulation,[54] of which its decrease triggers mood disorders.[55] Hence, we examined 5-HT in brain tissue in mice. The outcome of the experiments, at variance with the results of DZP treatment, indicated an elevation of 5-HT concentrations in the hippocampus and cerebral cortex, and the anxiolytic effect it exhibited correlated with the treatment with OD-CDs. In addition, a high dose of OD-CDs and DZP significantly increased the concentration of NE. Altered concentrations of 5-HT and NE may be the source of the anxiolytic effect of OD-CDs.

With the development of anxiety and depression, the HPA axis is activated and involved in the release of CRH from the hypothalamus, which initiates the release of ACTH from the pituitary, ultimately resulting in CORT release from the adrenal gland in mice.[56–58] The concentration of CRH can increase with acute and chronic stress and anxiolytic drugs can reverse this phenomenon.[59] In addition, the synthesis and release of neurotransmitters and the levels of CRH, ATCH, and CORT have been linked to neuropsychiatric disorders. The high-dose OD-CDs significantly decreased the concentrations of CRH, ACTH, and CORT, further supporting the inference that OD-CDs impact the HPA axis.

The anxiolytic effect of OD-CDs, a nanomaterial found in Os Draconis, has been verified by the experimental results of this study, which can partially clarify the basis of the pharmacological effect of Os Draconis, whereas further exploration and research are needed to identify how OD-CDs interact with various hormones and neurotransmitters in the HPA axis.

Conclusion

This study is the first to identify carbon nanocomponents from Os Draconis. Four behavioural tests (OFT, LDT, EPMT, and NSFT) revealed a significant anxiolytic effect of OD-CDs treatment in mic. Meanwhile, this finding indicates that OD-CDs partly mediate the regulation of monoaminergic neurotransmitters and the HPA axis. Furthermore, these effects may be mediated by monoaminergic neurotransmitters and the HPA axis but specific mechanisms need to be explored more concretely. Because of OD-CDs definite anxiolytic effect, it provides support for developing OD-CDs as a new anti-anxiety drug and deserves further study.

Acknowledgments

We greatly appreciate the support of the Special Funds for Fundamental Research Expenses of Central Universities (China). In addition, we acknowledge the support of the Classical Prescription Basic Research Team of Beijing University of Chinese Medicine and the Key Laboratory of Behavioural tests of Center of Scientific Experiment, School of Basic Medical Sciences.

Disclosure

The authors report no conflicts of interest in this work.

References

1. Rapee RM, Schniering CA, Hudson JL. Anxiety disorders during childhood and adolescence: origins and treatment. *Annu Rev Clin Psychol*. 2009;5(1):311–341. doi:10.1146/annurev.clinpsy.032408.153628
2. Mclean CP, Asnaani A, Litz BT, Hofmann SG. Gender differences in anxiety disorders: prevalence, course of illness, comorbidity and burden of illness. *J Psychiatr Res*. 2011;45(8):1027–1035. doi:10.1016/j.jpsychires.2011.03.006
3. Baxter AJ, Scott KM, Vos T, Whiteford HA. Global prevalence of anxiety disorders: a systematic review and meta-regression. *Psychol Med*. 2013;43(5):897–910.
4. James SL, Abate D, Abate KH, et al. Global, regional, and national incidence, prevalence, and years lived with disability for 354 diseases and injuries for 195 countries and territories, 1990–2017: a systematic analysis for the Global Burden of Disease Study 2017. *Lancet*. 2018;392(10159):1789–1858.
5. Youssef NA, Rich CL. Does acute treatment with sedatives/hypnotics for anxiety in depressed patients affect suicide risk? A literature review. *Ann Clin Psychiatry*. 2008;20(3):157.

6. Bighelli I, Castellazzi M, Cipriani A, et al. Antidepressants versus placebo for panic disorder in adults. *Cochrane Database Syst Rev*. 2018;4:CD010676.
7. Penninx BW, Pine DS, Holmes EA, Reif A. Anxiety disorders. *Lancet*. 2021;397(10277):914–927.
8. Xu X, Ray R, Gu Y, et al. Electrophoretic analysis and purification of fluorescent single-walled carbon nanotube fragments. *J Am Chem Soc*. 2004;126(40):12736–12737.
9. Zhang M, Zhao Y, Cheng J, et al. Novel carbon dots derived from *Schizonepetae Herba Carbonisata* and investigation of their haemostatic efficacy. *Artif Cells, Nanomed Biotechnol*. 2017;1:12.
10. Yan X, Zhao Y, Luo J, et al. Hemostatic bioactivity of novel Pollen Typhae Carbonisata-derived carbon quantum dots. *J Nanobiotechnology*. 2017;15(1):60. doi:10.1186/s12951-017-0296-z
11. Liu X, Wang Y, Yan X, et al. Novel Phellodendri Cortex (Huang Bo)-derived carbon dots and their hemostatic effect. *Nanomedicine*. 2018;13(4):391–405. doi:10.2217/nnm-2017-0297
12. Lu F, Ma Y, Huang H, et al. Edible and highly biocompatible nanodots from natural plants for the treatment of stress gastric ulcers. *Nanoscale*. 2021;13(14):6809–6818. doi:10.1039/D1NR01099A
13. Zhang Y, Wang S, Lu F, et al. The neuroprotective effect of pretreatment with carbon dots from *Crinis Carbonisatus* (carbonized human hair) against cerebral ischemia reperfusion injury. *J Nanobiotechnology*. 2021;19(1):257. doi:10.1186/s12951-021-00908-2
14. Xue X, Yang J-Y, He Y, et al. Aggregated single-walled carbon nanotubes attenuate the behavioural and neurochemical effects of methamphetamine in mice. *Nat Nanotechnol*. 2016;11(7):613–620. doi:10.1038/nnano.2016.23
15. Eidi H, David MO, Crepeaux G, et al. Fluorescent nanodiamonds as a relevant tag for the assessment of alum adjuvant particle biodisposition. *BMC Med*. 2015;13(1):144. doi:10.1186/s12916-015-0388-2
16. Alawdi SH, El-Denshary ES, Safar MM, Eidi H, David MO, Abdel-Wahhab MA. Neuroprotective effect of nanodiamond in Alzheimer's disease rat model: a pivotal role for modulating NF-κB and STAT3 signaling. *Mol Neurobiol*. 2017;54(3):1906–1918. doi:10.1007/s12035-016-9762-0
17. Xu WW, Du JN, Hao XL, Ni Y, Ji HX, Yang WH. Modern research and application of Long gu. *Zhongguo Zhong Yao Za Zhi*. 2017;42(10):1825–1829. doi:10.19540/j.cnki.cjcmm.20170224.016
18. Ha JH, Lee MG, Chang SM, Lee JT. In vivo characterization of sedative activities of Fossilia Mastodi OSSIS. *Biol Pharm Bull*. 2006;29(7):1414–1417. doi:10.1248/bpb.29.1414
19. Zhang H, Zhang L, Liu Y. Studies on chemical components and pharmacological activities of Os Draconis (Longgu) and Ostreae Concha. *Zhongguo Zhong Yao Za Zhi*. 2011;36(13):1839–1840.
20. Yang L, Jiang W, Qiu L, et al. One pot synthesis of highly luminescent polyethylene glycol anchored carbon dots functionalized with a nuclear localization signal peptide for cell nucleus imaging. *Nanoscale*. 2015;7(14):6104–6113. doi:10.1039/C5NR01080B
21. Carola V, D'Olimpio F, Brunamonti E, Mangia F, Renzi P. Evaluation of the elevated plus-maze and open-field tests for the assessment of anxiety-related behaviour in inbred mice. *Behav Brain Res*. 2002;134(1–2):49. doi:10.1016/S0166-4328(01)00452-1
22. Saitoh A, Kimura Y, Suzuki T, Kawai K, Nagase H, Kamei J. Potential anxiolytic and antidepressant-like activities of SNC80, a selective delta-opioid agonist, in behavioral models in rodents. *J Pharmacol Sci*. 2004;95(3):374–380. doi:10.1254/jphs.FPJ04014X
23. Lister RG. Ethologically-based animal models of anxiety disorders. *Pharmacol Ther*. 1990;46(3):321.
24. Young R, Johnson DN. Comparison of routes of administration and time course effects of zacopride and buspirone in mice using an automated light/dark test. *Pharmacol Biochem Behav*. 1991;40(4):733–737.
25. Piato AL, Detanico BC, Linck VM, Herrmann AP, Nunes DS, Elisabetsky E. Anti-stress effects of the "tonic"*Ptychopetalum olacoides* (Marapuama) in mice. *Phytomedicine*. 2010;17(3):248–253.
26. Guo JY, Yuan XY, Sui F, et al. Placebo analgesia affects the behavioral despair tests and hormonal secretions in mice. *Psychopharmacology*. 2011;217(1):83–90.
27. David DJ, Samuels BA, Rainer Q, et al. Neurogenesis-dependent and -independent effects of fluoxetine in an animal model of anxiety/depression. *Neuron*. 2009;62(4):479–493.
28. Shephard RA, Broadhurst PL. Hyponeophagia in the Roman rat strains: effects of 5-methoxy-N, N-dimethyltryptamine, diazepam, methysergide and the stereoisomers of propranolol. *Psychopharmacology*. 1982;78(4):368–372.
29. Jia P, Yu L, Tao C, Dai G, Zhang Z, Liu S. Chitosan oligosaccharides protect nucleus pulposus cells from hydrogen peroxide-induced apoptosis in a rat experimental model. *Biomed Pharmacother*. 2017;93:807–815.
30. Wang L, Bi YD, Hou J, et al. Facile, green and clean one-step synthesis of carbon dots from wool: application as a sensor for glyphosate detection based on the inner filter effect. *Talanta*. 2016;160:268–275.
31. Cutrim ESM, Vale AAM, Manzani D, et al. Preparation, characterization and in vitro anticancer performance of nanoconjugate based on carbon quantum dots and 5-Fluorouracil. *Mater Sci Eng C Mater Biol Appl*. 2021;120:111781.
32. Shen J, Shang SM, Chen XY, Wang D, Cai Y. Highly fluorescent N, S-co-doped carbon dots and their potential applications as antioxidants and sensitive probes for Cr (VI) detection. *Sensor Actuat B-Chem*. 2017;248:92–100.
33. Atchudan R, Edison T, Aseer KR, Perumal S, Karthik N, Lee YR. Highly fluorescent nitrogen-doped carbon dots derived from *Phyllanthus acidus* utilized as a fluorescent probe for label-free selective detection of Fe^{3+} ions, live cell imaging and fluorescent ink. *Biosens Bioelectron*. 2018;99:303–311.
34. Uskokovic V. X-ray photoelectron and ion scattering spectroscopic surface analyses of amorphous and crystalline calcium phosphate nanoparticles with different chemical histories. *Phys Chem Chem Phys*. 2020;22(10):5531–5547.
35. Chen YuZhi LS. Analysis of components in Os Draconis and Oyster Shells. *J Fujian Med Univ*. 1999;3(04):432–434.
36. Cappell H, Le BA. Punishment of saccharin drinking by amphetamine in rats and its reversal by chlordiazepoxide. *J Comp Physiol Psychol*. 1973;85(1):97–104.
37. Griebel G, Holmes A. 50 years of hurdles and hope in anxiolytic drug discovery. *Nat Rev Drug Discov*. 2013;12(9):667–687.
38. Bourin M. Animal models for screening anxiolytic-like drugs: a perspective. *Dialogues Clin Neuro*. 2015;17(3):295–303.
39. Panayotis N, Freund PA, Marvaldi L, et al. β-sitosterol reduces anxiety and synergizes with established anxiolytic drugs in mice. *Cell Rep Med*. 2021;2:5.
40. Santos P, Herrmann AP, Benvenutti R, et al. Anxiolytic properties of *N*-acetylcysteine in mice. *Behav Brain Res*. 2017;317:461–469.

41. Liu J, Lv YW, Shi JL, et al. Anti-anxiety effect of (−)-Syringaresnol-4-O-β-D-apiofuranosyl-(1→2)-β-D-glucopyranoside from *Albizzia julibrissin* Durazz (Leguminosae). *Molecules*. 2017;22:8.
42. Richter L, de Graaf C, Sieghart W, et al. Diazepam-bound GABAA receptor models identify new benzodiazepine binding-site ligands. *Nat Chem Biol*. 2012;8(5):455–464.
43. Liu J, Zhai WM, Yang YX, et al. GABA and 5-HT systems are implicated in the anxiolytic-like effect of spinosin in mice. *Pharmacol Biochem Behav*. 2015;128:41–49.
44. Feng XR, Xu WG, Li ZM, Song WT, Ding JX, Chen XS. Immunomodulatory Nanosystems. *Adv Sci*. 2019;6(17):32.
45. Ren CX, Hu XG, Zhou QX. Graphene oxide quantum dots reduce oxidative stress and inhibit neurotoxicity in vitro and in vivo through catalase-like activity and metabolic regulation. *Adv Sci*. 2018;5:5.
46. Pan H, Sun T, Cui M, et al. Light-SENSITIVE *Lactococcus lactis* for microbe-gut-brain axis regulating via upconversion optogenetic micro-nano system. *ACS Nano*. 2022;3:12.
47. Siyal FJ, Siddiqui RA, Memon Z, et al. Eugenol and its liposome-based nano carrier reduce anxiety by inhibiting glyoxylase-1 expression in mice. *Braz J Biol*. 2021;83:e251219.
48. Spaull R, McPherson B, Gialeli A, et al. Exosomes populate the cerebrospinal fluid of preterm infants with post-haemorrhagic hydrocephalus. *Int J Dev Neurosci*. 2019;73:59–65.
49. Kim HY, Kumar H, Jo MJ, et al. Therapeutic efficacy-potentiated and diseased organ-targeting nanovesicles derived from mesenchymal stem cells for spinal cord injury treatment. *Nano Lett*. 2018;18(8):4965–4975.
50. Lai RC, Yeo RW, Tan KH, Lim SK. Exosomes for drug delivery - a novel application for the mesenchymal stem cell. *Biotechnol Adv*. 2013;31(5):543–551.
51. Faravelli C, Lo SC, Lelli L, et al. The role of life events and HPA axis in anxiety disorders: a review. *Curr Pharm Des*. 2012;18(35):23.
52. Elhwuegi AS. Central monoamines and their role in major depression. *Prog Neuropsychopharmacol Biol Psychiatry*. 2004;28(3):435–451.
53. Krishnan V, Nestler EJ. The molecular neurobiology of depression. *Nature*. 2008;455(7215):894–902.
54. Andrews PW, Bharwani A, Lee KR, Fox M, Thomson JA Jr. Is serotonin an upper or a downer? The evolution of the serotonergic system and its role in depression and the antidepressant response. *Neurosci Biobehav Rev*. 2015;51:164–188.
55. Li H, Liu Y, Gao X, et al. Neuroplastin 65 modulates anxiety- and depression-like behavior likely through adult hippocampal neurogenesis and central 5-HT activity. *FEBS J*. 2019;286(17):3401–3415.
56. Locatelli V, Bresciani E, Tamiazzo L, Torsello A. Central nervous system-acting drugs influencing hypothalamic-pituitary-adrenal axis function. *Endocr Dev*. 2010;17:108–120.
57. Onoue Y, Kuwatsuka K, Miyazaki I, Asanuma M, Kitamura Y, Sendo T. Effects of bupropion and pramipexole on cell proliferation in the hippocampus of adrenocorticotropic hormone-treated rats. *Biol Pharm Bull*. 2014;37(2):327–330.
58. McKay MS, Zakzanis KK. The impact of treatment on HPA axis activity in unipolar major depression. *J Psychiatr Res*. 2010;44(3):183–192.
59. Van Bockstaele EJ, Colago EE, Valentino RJ. Corticotropin-releasing factor-containing axon terminals synapse onto catecholamine dendrites and may presynaptically modulate other afferents in the rostral pole of the nucleus locus coeruleus in the rat brain. *J Comp Neurol*. 1996;364(3):523–534.